

Implementation of an XPW filter at the LOASIS laser system

5.1 Introduction

In the third and fourth chapter of this manuscript the nonlinear process of XPW generation has been introduced theoretically and experimentally. In the present chapter all the results and conclusions that have been reached so far are used for the practical implementation of an XPW contrast filter to improve the temporal contrast of the Lasers, Optical, Accelerator Systems Integrated Studies (LOASIS) laser facility at the Lawrence Berkeley National Laboratory (LBNL) in Berkeley (Ca, USA). This work was done in collaboration with O. Albert who spent one year as a visiting scientist in the LOASIS group lead by Dr. Wim Leemans. My collaboration with LOASIS was part of my Ph.D grant (Bourse Monge, Ecole Polytechnique). This grant involves spending 6 weeks as a visiting scientist in a foreign laboratory.

5.2 Influence of the temporal contrast on electron acceleration

In chapter 2 I explained the importance of a high temporal contrast for avoiding pre-ionization of matter, in particular for high order harmonic generation on solid target. Solid targets are also used for proton acceleration and a high temporal contrast of the pulses is needed for efficient acceleration with thin targets [4]. The temporal quality of the pulses is also important in the interaction of a high intensity pulse with a gas jet as is the case for electron acceleration [8, 5]. Laser-based wakefield electron accelerators recently become the subject of vigorous investigation in many laboratories, mostly because of their potential as compact sources of high energy electron beams and bright, ultra-short pulse light sources for fundamental studies [1, 3, 7, 2, 6]. It has been revealed that the fine details of the optical properties of the driving laser pulses, such as pulse shape [5] and pre-pulse contrast [8], have significant effects on the properties and usability of the generated electron beams. In particular, the forward-running part of a high

intensity, ultrashort laser pulse, (pre-pulse or ASE pedestal) could start ionizing (or at least start modifying the index of refraction) the interaction medium in a plasma accelerator and eventually disturb the plasma wake generation process.

As presented in section 2.2.2, pulses with a temporal (ns) contrast of 6-7 order of magnitude with possible pre-pulses are typical in most CPA laser systems. Therefore, in order to improve the stability of laser plasma accelerators, there is a strong need to improve the contrast of the driver laser pulses. The solution selected for improving the contrast of the LOASIS laser facility is the implementation of an XPW contrast filter in a double CPA configuration.

5.3 Implementation of the XPW filter at the LOASIS laser system

The first implementation of an XPW filter in a double CPA configuration was realized at the Laboratoire d'Optique Appliquée. The XPW filter was designed to filter 1 mJ pulses in a double crystal configuration (two [100] BaF_2 crystals of 2 mm, first crystal in the focus), with an expected output energy of several hundreds of μJ . These filtered pulses are then stretched and amplified in several multi-pass amplifiers up to the joule level. The schematic of this filter is shown in Fig. 5.1. The practical realization of this filter has demonstrated several limitations in daily operation. First, the distance between the two crystals to avoid white-light generation or damaging in the second crystal was underestimated. Therefore, to keep the distance between the crystals acceptable for the vacuum chamber, the input energy is limited to 300 μJ with an output of just some tens of μJ . The distance between the crystals for filtering 1 mJ at 30 fs with the current input beam size is 1 meter. Second the size of the vacuum chamber (all the system is under vacuum) and the weight of the cover make the system not easy for daily alignment. Starting with these considerations it was decided, for the implementation in the LOASIS laser, to limit the input energy to 300 μJ and to work in air. Working in air is favorable in this case due to the relatively long duration of the pulses (45 fs) injected into the filter. A single double-passed [101]-cut BaF_2 crystal located in the focus is used for maximizing the efficiency and to make the system more robust to variations of the input intensity.

The LOASIS laser before the upgrade is presented in Fig. 5.2 top. The inclusion of the XPW pre-pulse filter required the installation of 4 new building blocks into the existing CPA laser chain (Fig. 5.2 bottom):

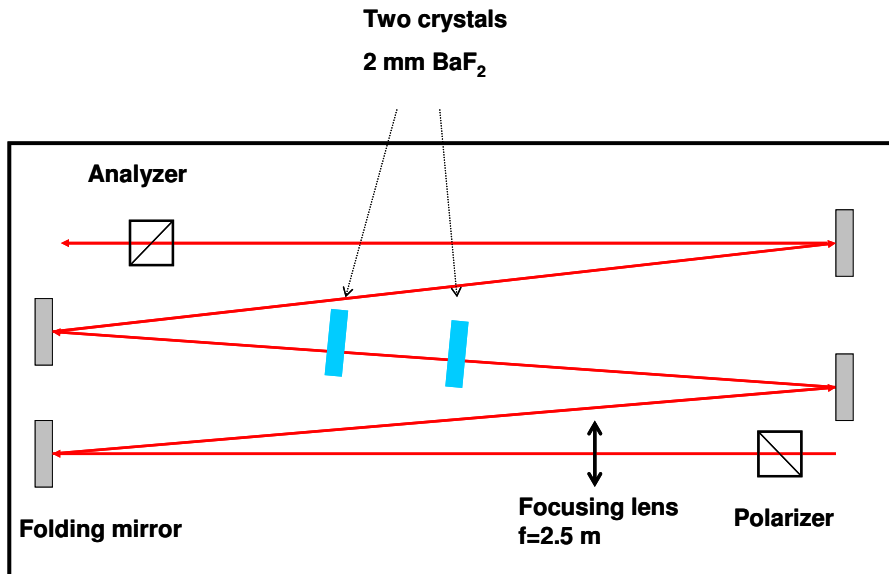


Figure 5.1: Schematic of the XPW filter installed at LOA (salle jaune) for the contrast enhancement in a double CPA configuration

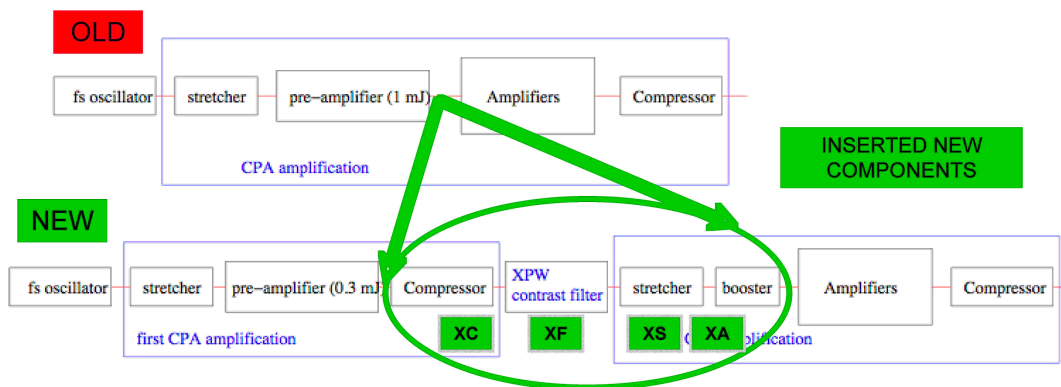


Figure 5.2: Front end of the LOASIS CPA system with the new components (see text for details)

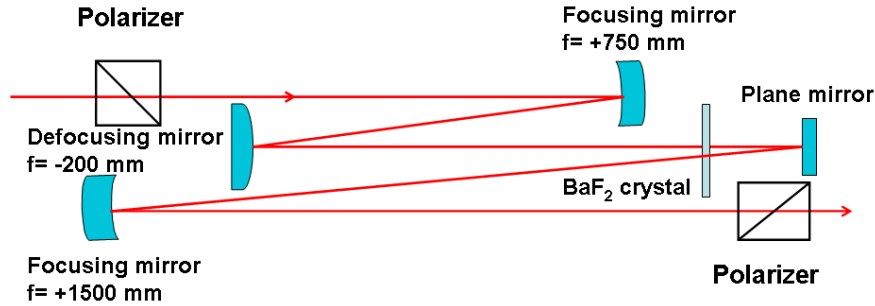


Figure 5.3: Schematic of the XPW filter implemented at the LOASIS laser facility. It comprises of the two, high extinction ratio (10^5) crossed polarizers, three curved optics forming a 4 m focal length focusing telescope in order to appropriately match the beam size in the BaF_2 nonlinear crystal, and a folding mirror to provide double path in the nonlinear crystal and also helping to maintain a compact foot-print ($1.5 \times 0.2 \text{ m}^2$) for the whole setup. All components are situated in air

- XC: XPW compressor. For the correct functioning of the filter the normally stretched pulse (220 ps) needs to be compressed. A compressor part of a commercial (Newport/Spectra Physics) Stretcher/Compressor system with 1500 line/mm groove density and with a matched angle of incidence to the LOASIS CPA system was used.
- XF: The XPW filter itself (Fig. 5.3). It consists of two, high extinction ratio (10^5), calcite crossed polarizers, two curved optics forming a 4 m focal length focusing telescope in order to appropriately match the beam size in the BaF_2 nonlinear crystal (located in the focus), and a folding mirror to provide double passing of the nonlinear crystal and also help maintain a compact foot-print ($1.5 \times 0.2 \text{ m}^2$) for the whole setup. After the second pass in the crystal the beam is collimated with a $f=+1500 \text{ mm}$ focusing mirror
- XS: XPW stretcher. The filtered pulse has to be stretched again back to $220\text{-}250 \text{ ps}$ to be ready for further amplification in the CPA chain. Here we used the stretcher part of a commercial (Newport/Spectra Physics) Stretcher/Compressor system with 1100 line/mm groove density and matched angle of incidence to the LOASIS CPA system.
- XA: XPW amplifier. This is a multipass booster amplifier, that makes up the losses in the previous three components, and brings back up the energy of the pulses from $30 \mu\text{J}$ to 1 mJ , the same energy level, as before the insertion of the XPW filter system. In order to preserve the achieved contrast enhancement in the XF and to avoid ASE build-up

during the amplification process, the pump fluence in the Ti:Sa amplifier crystal is kept below 1.4 J/cm^2 and the number of passes was also kept low. A balanced 4-pass system was designed using the Frantz-Nodvik laser amplifier model. A flashlamp pumped and intracavity doubled, 10 Hz, 300 mW average power Nd:YAG laser ('ULTRA' from Big Sky Lasers) was used as the pumping source. The actual pump fluence was controlled by an external polarizer/waveplate setup.

The cleaned pulses are re-amplified to 40 mJ, then split to seed three independent amplifiers forming a multiple second CPA. The beam energy of the first power amplifier reaches 1 J, while the second amplifier's output (0.9 J) is split again to provide independently compressed beams for multi-beam plasma channel experiments. The third, cryo-cooled power amplifier produces 3.8 J/pulse at 10 Hz repetition rate, and propagates in vacuum tubes to the radiation shielded experimental area for final compression (35 fs). This beam is used in a capillary discharge plasma target area

The summary of the energy and spectral parameters of the laser beam measured after the installation of the XPW filter are:

- input/output energy to/from XPW filter (XF): 250-300 μJ / 30-70 μJ .
- input/output optical spectrum FWHM at XPW filter: 46 nm/53 nm (Fig. 5.5a).

The contrast enhancement factor, at different time regions before the arrival of the main pulse, was measured using a commercial third-order cross-correlator device ('Sequoia' from Amplitude Technologies, Inc.). The first measurement (Fig. 5.4) was performed inside the laser chain after the booster amplifier (energy 1 mJ). To make this measurement possible the stretched beam (220 ps) is roughly compressed in a gratings compressor. The second measurement (Fig. 5.5b) was performed at the output of the 100 TW system. In the first measurement an increase in incoherent contrast by at least 3 orders of magnitude is visible. This is less than the extinction ratio of the crossed polarizers. We believe that this is due to a stress induced linear birefringence in the BaF_2 crystal. From the correlation trace the coherent pedestal due to the imperfect compression is also clearly visible. The coherent contrast is cleaned just after XPW and this residual spectral phase is due to the rough compression. This coherent contrast can be reduced by an accurate compression and by measuring accurately the spectral phase at the end of the laser chain and, with a feedback loop, compensate it with a pulse shaper. This issue will be addressed in section 6.3. At the output of the laser chain (Fig. 5.5b) the contrast enhancement is from 10^{-6} to 10^{-9} for the pedestal region, and from 10^{-4} to 10^{-8} for the prepulses at -5 ps time delay. The decrease in incoherent contrast compared to the measurement inside the laser system is due to the further amplification to the joule level.

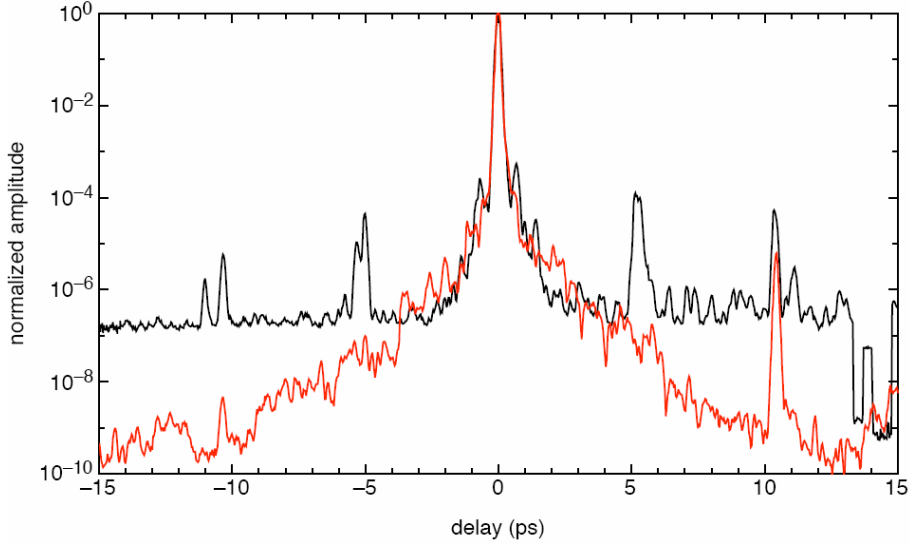


Figure 5.4: Sequoia measurement just after the XA amplifier and a rough recompression

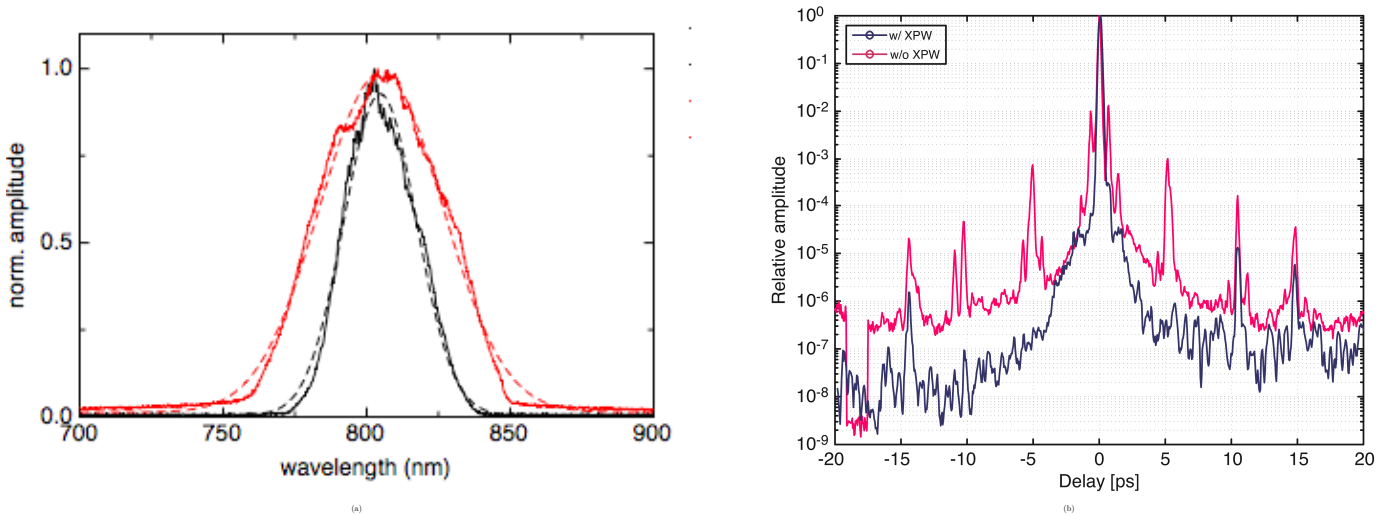


Figure 5.5: (a): Optical spectrum measured by an Ocean Optics 4000 USB spectrometer. The narrow, black curve is the input, and the broader, red curve represents the output of the XPW filter. Dashed lines are Gaussian fits to determine FWHM values. (b): Sequoia measurement data. The upper, red curve is the input, and the lower, blue curve represents the output of the XPW filter.

5.4 Improvements after the installation of the XPW filter

After the installation of the XPW filter, significant improvements of various characteristics of the laser beam along the amplifier chain and that of the generated electron and secondary radiation beams have been observed. Here I present two particular examples:

- enhanced yield and more stable THz emission from gas jet e-beam/THz experiments performed at the 10 TW laser beam line
- improved pointing and amplitude stability of the main 100 TW laser ('TRex') beam line used to generate GeV electron beams in capillary guided laser plasma accelerator experiments

5.4.1 Improvements of THz emission

As one of the potential future applications of laser wakefield accelerators, LWFAs, and also as a useful diagnostic tool for the accelerated electron bunches of these same LWFAs, the LOASIS group has extensively studied the intense THz emission phenomenon observed at the exit boundary of the plasma region in a typical gas-jet style LWFA experiment [9]. The laser pulses interacting with the plasma create accelerated electrons, which upon exiting the plasma emit THz pulses via transition radiation. Because these electron bunches are ultrashort (<50 fs), they can radiate coherently (coherent transition radiation - CTR) over a wide bandwidth (1 - 10 THz) yielding high intensity THz pulses [9]. In addition to providing a non-invasive bunch-length diagnostic and thus feedback for the LWFA, these high peak power THz pulses are suitable for high field (MV/cm) pump-probe experiments. In order to further understand the physical processes taking place in the interaction region, stable laser and electron beams are necessary for detailed parameter-scan experiments. For example, a typical, widely used scan is the "compressor scan", in which the grating separation of the last compressor is changed to tune the temporal duration of the compressed pulses. Fig. 5.6 shows an example of this scan where the total electron bunch charge is measured as a function of the grating separation. The two curves correspond to before (red) and after (blue) the installation of the XPW filter. An increase (4 times) of the total electron bunch charge is visible after the installation of the filter. Furthermore, the relative fluctuation of the charge (represented by the error bars) has also improved, resulting in dramatic improvements in the THz signal amplitude stability. The shot-to-shot variation, which were at the 100 % level prior to XPW implementation, decreased to the 10 % level. Similar improvements were observed for the gamma and neutron yields, constantly monitored during the experiments for radiation protection purposes.

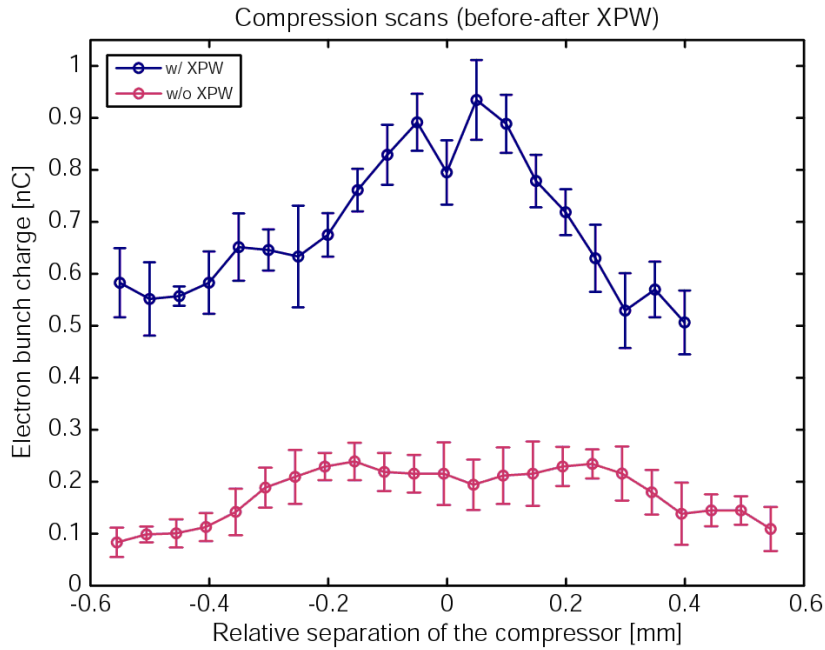


Figure 5.6: Comparison of total emitted bunch charge in a LWFA experimental compressor scan before (lower, red curve) and after (upper, blue curve) the installation of the XPW prepulse filter

5.4.2 Laser beam stability improvements

Since the XPW filtering process effectively improves both the spatial mode profile and spectral stability one can expect an overall improvement of the statistical parameters of the CPA laser. The amplitude and pointing stability variations of the laser beam have been recorded in the TRex (nominal 100 TW) laser beam line. A 3% RMS. energy variation was measured in a set of 200 shots at 1.5 J average energy on target in each pulse, and $2.5 \mu\text{rad}$ RMS pointing stability in a $f = 2 \text{ m}$ focusing geometry with $25 \mu\text{m}$ focal spot (Fig. 5.7). (Previous values were 5% energy stability and $10 \mu\text{rad}$ r.m.s pointing stability.) These improvements are crucial for production of stable GeV electron in capillary discharges.

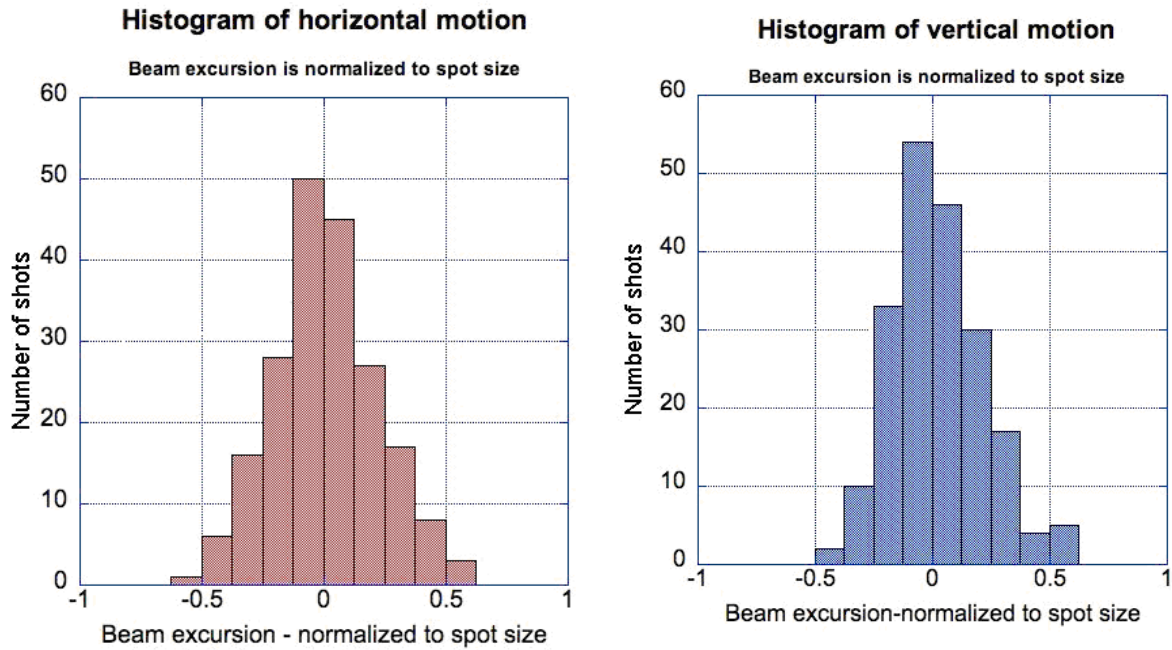


Figure 5.7: Horizontal (a) and vertical(b) pointing stability of the 100 TW beam line after installation of the XPW filter

Bibliography

- [1] J. Faure, Y. Glinec, A. Pukhov, S. Kiselev, S. Gordienko, E. Lefebvre, J.-P. Rousseau, F. Burgy, and V. Malka. A laser-plasma accelerator producing monoenergetic electron beams. *Nature*, 431(7008):541–544, September 2004.
- [2] J. Faure, C. Rechatin, A. Norlin, A. Lifschitz, Y. Glinec, and V. Malka. Controlled injection and acceleration of electrons in plasma wakefields by colliding laser pulses. *Nature*, 444(7120):737–739, December 2006.
- [3] C. G. R. Geddes, Cs. Toth, J. van Tilborg, E. Esarey, C. B. Schroeder, D. Bruhwiler, C. Nieter, J. Cary, and W. P. Leemans. High-quality electron beams from a laser wakefield accelerator using plasma-channel guiding. *Nature*, 431(7008):538–541, September 2004.
- [4] M. Kaluza, J. Schreiber, M. I. K. Santala, G. D. Tsakiris, K. Eidmann, J. Meyer-ter Vehn, and K. J. Witte. Influence of the laser prepulse on proton acceleration in thin-foil experiments. *Phys. Rev. Lett.*, 93(4):045003–, July 2004.
- [5] W. P. Leemans, P. Catravas, E. Esarey, C. G. R. Geddes, C. Toth, R. Trines, C. B. Schroeder, B. A. Shadwick, J. van Tilborg, and J. Faure. Electron-yield enhancement

- in a laser-wakefield accelerator driven by asymmetric laser pulses. *Phys. Rev. Lett.*, 89(17):174802, Oct 2002.
- [6] W. P. Leemans, B. Nagler, A. J. Gonsalves, Cs. Toth, K. Nakamura, C. G. R. Geddes, E. Esarey, C. B. Schroeder, and S. M. Hooker. GeV electron beams from a centimetre-scale accelerator. *Nat Phys*, 2(10):696–699, October 2006.
- [7] S. P. D. Mangles, C. D. Murphy, Z. Najmudin, A. G. R. Thomas, J. L. Collier, A. E. Dangor, E. J. Divall, P. S. Foster, J. G. Gallacher, C. J. Hooker, D. A. Jaroszynski, A. J. Langley, W. B. Mori, P. A. Norreys, F. S. Tsung, R. Viskup, B. R. Walton, and K. Krushelnick. Monoenergetic beams of relativistic electrons from intense laser-plasma interactions. *Nature*, 431(7008):535–538, September 2004.
- [8] S P D Mangles, A G R Thomas, M C Kaluza, O Lundh, F Lindau, A Persson, Z Najmudin, C-G Wahlstrom, C D Murphy, C Kamperidis, K L Lancaster, E Divall, and K Krushelnick. Effect of laser contrast ratio on electron beam stability in laser wakefield acceleration experiments. *Plasma Physics and Controlled Fusion*, 48(12B):B83–B90, 2006.
- [9] J. van Tilborg, C. B. Schroeder, C. V. Filip, Cs. Toth, C. G. R. Geddes, G. Fubiani, R. Huber, R. A. Kaindl, E. Esarey, and W. P. Leemans. Temporal characterization of femtosecond laser-plasma-accelerated electron bunches using terahertz radiation. *Physical Review Letters*, 96(1):014801, 2006.